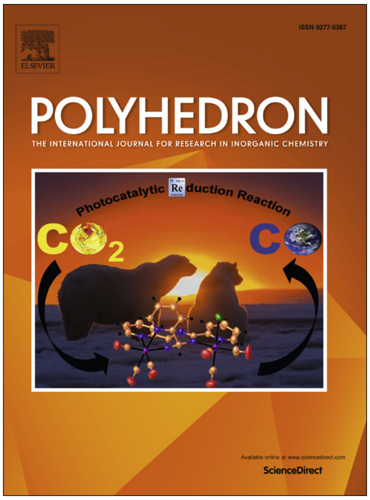

Dielectric properties induced by the framework in the hybrid organic-inorganic compounds $M(dca)_2pyz$ M=Fe, Co and Zn

A. García-Fernández, J.M. Bermúdez-García, S. Castro-García, R. Artiaga, J. López-Beceiro, M.A. Señarís-Rodríguez, M. Sánchez-Andújar

PII: S0277-5387(15)00777-9
DOI: http://dx.doi.org/10.1016/j.poly.2015.12.027
Reference: POLY 11726

To appear in: *Polyhedron*

Received Date: 28 September 2015
Accepted Date: 14 December 2015

Please cite this article as: A. García-Fernández, J.M. Bermúdez-García, S. Castro-García, R. Artiaga, J. López-Beceiro, M.A. Señarís-Rodríguez, M. Sánchez-Andújar, Dielectric properties induced by the framework in the hybrid organic-inorganic compounds $M(dca)_2pyz$ M=Fe, Co and Zn, *Polyhedron* (2015), doi: http://dx.doi.org/10.1016/j.poly.2015.12.027

Dielectric properties induced by the framework in the hybrid organic-inorganic compounds M(dca)$_2$pyz M=Fe, Co and Zn

A. García-Fernández[1], J. M. Bermúdez-García[1], S. Castro-García[1], R. Artiaga[2], J. López-Beceiro[2], M. A. Señarís-Rodríguez[1] and M. Sánchez-Andújar*[1]

[1]QuiMolMat Group, Department of Fundamental Chemistry, Faculty of Science and CICA, University of A Coruña, Campus A Coruña, 15071 A Coruña, Spain.

[2] Department of Industrial Engineering II, University of ACoruña. Campus Ferrol, 15403 Ferrol, Spain.

*corresponding author: Tel.: (+34) 981167000 e-mail: msanchez@udc.es

Abstract

In this work we prepare and study the M(dca)$_2$pyz compounds, where dca= polar dicyanamide $N(CN)_2^-$ ligand, pyz=pyrazine ($C_4H_4N_2$) ligand and M= Fe^{2+}, Co^{2+} and Zn^{2+} that, according to DSC display a first order phase transition, at T_t ~270 K (Fe), ~250 K (Co) and ~240 K (Zn). Very interestingly these compounds, which consist of a rather robust framework with incorporated polar dca ligands, and which does not host guest species in the cavities of the structure, display a dielectric anomaly associated to such phase transition. This latter in fact corresponds to the structural transition from the disordered HT-phase (space group *Pnma*) to the ordered LT-phase (space group $P2_1/n$). From a detailed analysis of the dipole distributions in each of these crystal structures we conclude that the polar dca ligands, which bridge two transition metal cations, display a cooperative electrical arrangement, in which the dipoles of each of the two interpenetrated networks show a ferroelectric (FE) arrangement; nevertheless, the relative antiparallel orientation of both networks finally results in net AFE arrangements both in the LT- and HT- polymorphs. Very interestingly, the dynamic disorder of the dca ligands at T_t gives rise to the observed dielectric anomaly. These materials constitute, therefore, an example of hybrid organic-inorganic compounds where the dielectric response directly arises from the framework –and not from polar guest species–, which is a very interesting and novel approach in the search for materials in which the dielectric and magnetic properties can couple more strongly.

Keywords: hybrid organic-inorganic materials, interpenetrated frameworks, phase transitions, dielectric properties, multiferroic materials.

Introduction

During the last years, the hybrid organic-inorganic frameworks with perovskite structure have attracted a great deal of attention and have made remarkable strides in different fields, such as photovoltaic solar cells [1], magnetic [2], dielectric [3] and even multiferroic materials [4].

Within this latter group, the hybrid perovskite compounds with cooperative electric and magnetic order continues to attract a lot of attention in view of the potential applications of such materials in many electric and electronic devices, like capacitors, temperature sensing, data storage, mechanical actuators, and so on [5,6].

Among them, the dense metal–organic frameworks (MOF) of formula $[A][M(HCOO)_3]$ (where A = mid-sized alkylammonium cations, such as methylammonium, ethylammonium, dimethylammonium, hydrazinium, formamidinium, cyclotrimethyleneammonium and imidazolium and M^{2+} = Mn^{2+}, Fe^{2+}, Co^{2+} and Ni^{2+}) are specially interesting as type I-multiferroics: they combine structural flexibility, relatively good stability, low density and cooperative magnetic and electrical properties [7-13]. These latter arise from different active ”subsystems”: i) A rather robust framework based on $[BO_6]$ octahedra, which are connected through the short organic formate ligands, and that displays cooperative magnetism at low temperatures (T_C: 8-36 K)[2]. ii) A polar mid-sized alkylammonium cations, that occupy the A-sites of the perovskite architecture, are linked to the framework via hydrogen bonds, and typically experience an order/disorder process that give rise to dielectric transitions [3,4,12] and even improper ferroelectricity [14]. In view of the different origins of the magnetic and ferroelectric order, weak direct magnetoelectric (ME) coupling should be expected in these systems.

Therefore, it would be very interesting to find alternative hybrid organic-inorganic materials where the dielectric and magnetic properties are driven by the same active subsystem as this would, in principle, facilitate a stronger coupling between the two ferroic properties.

In this context, the goal of this paper is to demonstrate that the framework of hybrid organic-inorganic materials can be responsible for both the magnetic and the dielectric properties in such type of materials.

For this purpose, we have looked up the literature in the search for a compound with the following features: a robust 3D framework with incorporated polar ligands and which does not host guest species in the cavities of the structure.

We have focused our attention in the $M(dca)_2pyz$ series of compounds, where members with M^{2+} = Mn^{2+}, Fe^{2+}, Co^{2+}, Ni^{2+}, Zn^{2+} and Cu^{2+}dca= polar dicyanamide $N(CN)_2^-$ ligand and pyz=pyrazine ($C_4H_4N_2$) ligand have been obtained and described [15]. From the structural point of view, these compounds contain two interpenetrating 3D ReO_3 related networks. Bidentate dca ligands, which have been widely used to synthesize a vast family of coordination polymers compounds [16,17], bridge the transition metal cations to form square-grid-like $M(dca)_2$ sheets, with the pyrazine ligands linking these sheets together to form the 3D networks, see Fig. 1 and more details at Fig. S1 of Supporting Information (S.I.) [15].

It is known that at room temperature, the crystal structure of these compounds is orthorhombic with space group *Pnma* and contains dynamic disorder of the dca and pyrazine ligands, see Fig. 1a and Fig. S1 of S.I.) [15]. Meanwhile, at lower temperatures the structure is monoclinic (space group $P2_1/n$) and the dca and pyrazine ligands are ordered, see Fig. 1b and Fig. S1 of S.I.) [15], even if the temperature and characteristics of such phase transition has not been reported yet for any of those compounds.

As for their magnetic properties, a weak antiferromagnetic coupling between the transition metal cations has been detected in the Mn^{2+}-, Fe^{2+}-, Co^{2+}- and Ni^{2+}-compounds, with evidence of long range antiferromagnetic order below 2.7 K in the case of the Mn-one [15].

Here and for the first time, we study the dielectric response and thermal behavior of the $M(dca)_2pyz$ compounds with M^{2+} = Fe^{2+}, Co^{2+} and Zn^{2+}. As we will show below, we have found that these compounds display a dielectric anomaly at the same temperature at which the structural phase transition takes place. So, both phenomena are associated. The obtained results support our initial hypothesis that dielectric and magnetic order can be both induced in the framework of hybrid organic-inorganic materials, which is a very interesting and novel approach to try to set a stronger coupling between the magnetic and dielectric properties.

Experimental Section

Materials

Iron (II) perchlorate hexahydrate $Fe(ClO_4)_2{\cdot}6{\cdot}H_2O$ (Merck 98%), cobalt (II) nitrate hexahydrate $Co(NO_3)_2{\cdot}6{\cdot}H_2O$ (Aldrich 98%), zinc (II) nitrate hexahydrate $Zn(NO_3)_2{\cdot}6{\cdot}H_2O$ (Aldrich 98%), sodium dicyanamide $NaN(CN)_2$ (Aldrich 96%) and pyrazine $CH_4H_4N_2$ (Aldrich 96%) were commercially available and used as purchased without further purification. A reagent amount of deionised water was also used in the synthesis.

Synthesis

The $M(dca)_2pyz$ where $M^{2+} = Fe^{2+}$, Co^{2+} and Zn^{2+}compounds were synthesized according to the procedure described in the literature [15]. In a typical experiment, a warm aqueous solution (5 mL) of $M(NO_3)_2{\cdot}xH_2O$ (0.6 mmol) was added to a warm aqueous solution (10 mL) of Na(dca) (1.2 mmol) and pyrazine (0.6 mmol). Fine crystals with needle morphology were obtained on cooling. They were washed with ethanol and dried at room temperature. They were found to be stable in air.

Elemental analysis

Elemental chemical analyses for C, N and H were carried out using a FLASHEA1112 (ThermoFinnigan) Analyzer.

For these compounds: Fe-compound calculated C: 35.85, H: 1.50, N: 41.81; found C: 35.95, H: 1.25, N: 40.68, Co-compound calculated C: 35.44, H: 1.49, N: 41.33; found C: 35.57, H: 1.21, N: 40.15, Zn-compound calculated C: 34.62, H: 1.45, N: 40.37; found C: 34.70, H: 1.15, N: 39.06.

Scanning Electron Microscopy

The morphology of the samples was studied by Scanning Electron Microscopy (SEM), in a JEOL 6400 microscope.

Powder X-ray diffraction

Powder X-ray diffraction (PXRD) at room temperature was performed in a Siemens D-5000 diffractometer using CuKα radiation (λ=1.5418 Å).

For the Fe- and Co-samples the typical holder was used for the experiments. Nevertheless, in the case of the Zn-sample, and in view of the very strong preferential orientation effects it displays (see below) a special procedure had to be used: first of all the sample had to be grinded during longer time (30 min) prior to deposit it onto a special sample holder, where the powder was sandwiched between two glasses to carry out the PXRD experiments.

The obtained PXRD patterns were analyzed by Le Bail profile analysis using the GSAS software [18]. The peak shapes were described by a pseudo-Voigt function and the background was modelled with a 6-term polynomial function.

Thermal studies

Thermogravimetric analyses (TGA) were carried out in a TGA-DTA Thermal Analysis SDT2960 equipment. For these experiments approximately 27 mg of sample were heated at a rate of 5 K/min from 300 K to 1200 K using corundum crucibles under a flow of dry nitrogen.

Differential scanning calorimetric (DSC) analyses were carried out in a TA Instruments MDSC Q-2000 equipped with a liquid nitrogen cooling system, by heating and cooling the sample during several cycles at 10 K/min up to 380 K under a nitrogen atmosphere.

Dielectric measurements

To measure the dielectric properties, pellets were prepared by cold pressing the obtained samples under a pressure of 10 tons that was maintained during 5 minutes. In addition, and taking into account that the compactness of the pellets can affect the dielectric properties their densities were determined by using the Archimedes method.

The complex dielectric permittivity ($\varepsilon_r = \varepsilon'_r - i\varepsilon''_r$) of the so obtained cold-press pelletized samples was measured as a function of frequency and temperature with a parallel-plate capacitor coupled to a Solartron1260A Impedance/Gain-Phase Analyzer, capable to measure in the frequency range from 10 μHz up to 32 MHz using an amplitude of 2 V. The capacitor was mounted in a Janis SVT200T cryostat refrigerated with liquid nitrogen, and with a Lakeshore 332 incorporated to control the temperature from 78K up to 400K. The data were collected on heating and before carrying out the measurements, the pellets were kept for two minutes at each temperature so as to reach the thermal equilibrium.

Pellets with an area of approximately 530 mm^2 and a thickness of approximately 1 mm were prepared to fit into the capacitor, and silver paste was painted on their surfaces to ensure a good electrical contact with the electrodes.

All the dielectric measurements were carried out in a nitrogen atmosphere where several cycles of vacuum and nitrogen gas were performed to ensure that the sample environment is free of water.

The impedance analysis software SMART (Solartron Analytical) was used for data acquisition and processing. Impedance complex plane plots were analyzed using the LEVM program, a particular program for complex nonlinear least squares fitting [19].

Results and discussion

General characterization

According to elemental chemical analyses for C, N and H, all the obtained materials have the expected chemical composition.

Although at first glance all the obtained crystals have a needle-like morphology, a more detailed analysis by SEM shows that these needles are in fact formed by stacking of sheets as it can be seen in Fig. 2, sheets that are very thin in the case of the Zn-sample.

These compounds were obtained as single phase materials, as confirmed by comparison of their experimental powder X-ray diffraction (PXRD) patterns at room temperature with those simulated from the corresponding single crystal X-ray diffraction data (SCXRD), see Fig. 3. We have to note that the intensity of several peaks in the experimental PXRD patterns do not match with the intensity of the simulated patterns. We suggest that this difference is due to the presence of preferential orientations in the samples, specially in the case of the Zn sample, related to the peculiar morphology of the crystals. In fact, in the case of this latter, and in order to try to minimize such effects in the PXRD patterns we had to follow a special procedure, to record them, as indicated in the Experimental section. In that context, it should be noted that the use of a special sample holder for that purpose help indeed to reduce the preferential orientation effects, even if it also resulted in a decrease in the intensity of the diffraction peaks , as it can be seen in Fig. 3 and S2 of S.I..

In addition, LeBail refinement of the obtained PXRD patterns indicates that at room temperature the three compounds show orthorhombic symmetry and space group *Pnma.* The obtained refinements are shown in Fig S2 and Table 1 summarizes the cell parameters obtained from such LeBail refinements for each compound. It should be indicated that these are in full agreement with those previously reported in the literature [15].

On the other hand, and in the case of the pellets obtained by cold-pressing and that will be used for the dielectric measurements, their experimental densities are in all cases very similar to the theoretical values, ~ 1.7 g/cm^3, that expressed as relative densities corresponds to~ 90 %.

Thermogravimetric analyses (TGA)

To study the thermal stability of the obtained materials, we have carried out thermogravimetric analyses under N_2 atmosphere. The thermal decomposition of the three compounds undergoes through a similar two-step weight loss, see Fig. 4.

The first weight loss (of 30.5-31.8 % depending on the compound) is due to the loss of all pyrazine ligands from the material. Meanwhile, the second weight loss (of 41-45.5 %, depending on the compound) is due to the partial removal of the dca ligands.

At temperatures above 1100º C the materials have completely decomposed into Co, Fe and ZnO, respectively, as revealed by the study of the XRPD patterns of the ashes obtained after the ATG experiment.

Differential scanning calorimetric (DSC)

As we have indicated in the Introduction, it has been reported that these compounds exhibit two polymorphs: a room temperature one and a low temperature one. Here, we have undertaken a DSC study to characterize the transition from one to another.

As shown in Fig. 5, according to the DSC results the three M(dca)$_2$pyz compounds display an endothermic peak on heating (that is seen at T_t ~277 K for M=Fe, ~ 250 K for M=Co and ~243 K for M=Zn) whose associated exothermic peak appears on cooling at T_t ~268 K when M=Fe, ~234 K when M=Co and ~238 K when M=Zn. Such transition seems to correspond to the structural phase transition from the orthorhombic polymorph (HT-phase) to the monoclinic one (LT-phase) [15].

The observed thermal hysteresis (see Fig. 5) implies that the transition is first order, as thermal hysteresis is thermodynamically forbidden in a second order transition [20].

The changes in the enthalpy ΔH (J mol^{-1}) and the entropy ΔS (J mol^{-1} K^{-1}) were determined from the area under the heat flow/time curves. The results, which depend on M as shown in detail in table S1 of S.I., yield enthalpies ΔH ~1100-1340 J mol^{-1} and entropies ΔS ~3.14-4.88 J mol^{-1} K^{-1}.

Taking into account that for an order-disorder transition $\Delta S = R \ln(N)$, where R is the gas constant and N is the ratio of the number of configurations in the disordered and ordered system, a value of N ~ 0.6 is calculated, for these compounds see table S1 of S.I..

In view of the LT- and HT-crystal structures [15], see Fig. 1, this value is much smaller than the one expected for this order-disorder phase transition, which implies at least fourfold order/disorder of the C-atoms of pyrazine and twofold order/disorder of the C- and N-amide atoms of the dca anions.

Also, the DCS results indicate that the order-disorder process takes place within a rather broad temperature range and is not an abrupt transition, as it is the case in other hybrid inorganic-organic materials, as for example in the $[(CH_3)_2NH_2][Mn(HCOO)_3]$ compound [21].

Dielectric properties

The temperature dependence of the real part of the complex dielectric permittivity, ε'_r, (the so-called dielectric constant) of these compounds was measured on a polycrystalline pellet at different frequencies. The obtained results are shown in Fig. 6.

A first general remark is that these compounds present a low dielectric constant value, which is frequency independent, except for the case of the Fe-compound, which displays a small frequency dependence for T>280 K.

Most interestingly, in the three compounds the ε'_r vs T curves display an anomaly, very close to the temperature at which the structural phase transition takes place, see Fig. 6. Also, in the temperature interval corresponding to the LT-phase, the ε'_r values are very small at low temperature and increase with temperature, showing a rather sharp rise close to the phase transition temperature (T_t). Just above T_t, and in the case of the Co- and Zn- compounds the dielectric constant goes through a broad maximum, and then the ε'_r values begin to slightly decrease. Meanwhile, in the case of the Fe-compound, a sharper rise in the dielectric constant is observed above the transition temperature in the HT-phase.

It should also be indicated that the observed anomalies in the ε'_r vs T curves are not as sharp as in other hybrid materials with dielectric properties [3,4,12]. This observation agrees with the DSC results, which indicate that the phase transition in the $M(dca)_2pyz$ ($M = Fe^{2+}$, Co^{2+} and Zn^{2+}) compounds is not abrupt and that the order-disorder process is taking place over a broad temperature range.

Taking into account that the presence of extrinsic factors such electronic and/or ionic conductivity could result in the appearance of artifacts in the dielectric measurements, we have made additional studies to make sure that the observed signal really comes from the sample.

For this purpose, and to avoid misinterpreting results[22,23] we have performed impedance complex plane (Z'' vs Z') analysis of the data obtained at different temperatures. A typical impedance complex plane plot for these samples in the whole temperature range 100<T(K)<350 K is shown in Fig. S3 of S.I.. This plot shows a single large arc that can be modeled by an equivalent circuit containing two elements connected in parallel: a resistance (R), and a capacitance (C). As this arc intercepts zero and the order of magnitude of its capacitance is of $pFcm^{-1}$ and the resistance is of giga Ω, it is associated with the material bulk response.[22] Taking into account that this is the only contribution present, we conclude that the observed dielectric response of these compounds is purely intrinsic and they are insulator in the whole studied temperature interval. This result confirms that the observed dielectric transition is real and associated to the material´s bulk response.

To understand the dielectric response of these compounds we have analysed in detail the characteristics of their LT- and HT-crystal structures, paying special attention to the spatial distribution of the dipole moments associated to the polar ligands.

For that purpose, we have focused in the arrangement of the polar dca ligand, which displays an electric dipole moment of μ=0.53 D, see Fig. S4 of S.I.. As these compounds are comprised of two interpenetrating networks, we will first refer to the dipole arrangement of one of the networks to subsequently check the arrangement of the whole structure.

In both the HT-phase and LT-phase, the dipole associated to the dca ligand displays a cooperative arrangement. Very interestingly, and as it can be seen in Fig. 7, the dipoles of each network show a ferroelectric (FE) arrangement along one of the crystal axis (that is the *a*-axis in the case of the HT-phase, that in fact correspond to the *b*-axis in the LT-polymorph).

Nevertheless, the antiparallel arrangement of the two interpenetrated FE networks finally gives rise to a net long-range antiferroelectric (AFE) order in both the HT- and LT-polymorphs of these compounds, see Fig. 7.

And the main different between the AFE arrangements in the two polymorphs relies on their "static" (in the LT-phase) or "dynamic" (in the HT-phase) characteristics. Such "static" vs "dynamic" nature is related to the order-disorder process that is experienced by the polar dca ligands at the structural phase transition.

In that context, the "dynamic" disorder of the dca ligands can sporadically break up the antiparallel arrangement of the electrical dipoles and be responsible for the dielectric anomaly observed at T_t. We have to note that this dielectric response has certain similarities with the behavior reported for the $(C_3N_2H_5)[Mn(HCOO)_3]$ metal–organic framework with perovskite–like structure [13]. In this compound, the $C_3N_2H_5^+$ imidazolium cations, which are guest cations located in the cavities of the framework, also display an antiferroelectric order that thermal energy seems to be able to sporadically break the antiparallel arrangement of the electrical dipoles, giving rise to the anomaly inε'_r vs T curve, in that case at T ~ 200K.

Thus, the origin of the dielectric anomaly observed in the here studied M(dca)$_2$pyz compounds (M= Fe, Co, Zn), is quite different from that observed in other hybrid inorganic-organic compounds, such as [A][M(HCOO)$_3$] (where A = mid-sized alkylammonium cations). In those latter the polar arrangement of the hybrid materials is typically related to order/disorder phenomena involving polar cations or to H-bonded between the framework and guest molecules, which are located inside the cavities of the framework. This is a drawback in order to obtain multiferroic materials with strong magnetoelectric coupling, due to the fact that the polar and magnetic order arise from different subunits: while the framework induces long range magnetic order and, the guest molecules provoke the polar arrangement. In the case of the here studied M(dca)$_2$pyz compounds, the dielectric response is directly provoked by their framework, as it is also their magnetic behavior in the case of the compounds containing transition metal ions with incomplete d orbitals.

This finding is very interesting and paves the way to obtain type II-multiferroic materials [24,25] based on hybrid organic-inorganic compounds, with a strong coupling between both functional properties.

Conclusions

We have prepared the M(dca)$_2$pyz with M^{2+} = Fe^{2+}, Co^{2+} and Zn^{2+} hybrid organic-inorganic compounds as single phase materials. These compounds are thermally stable up to T≈ 410 K-550 K depending of the transition metal cations, and their thermal decomposition occurs in two-steps. According to the DSC results, these compounds display a first order phase transition, that is seen at around ~270 K, ~250 K and ~240 K for the Fe, Co and Zn compounds, respectively, on heating and ~268 K, ~234 K and ~238 K for the Fe, Co and Zn compounds, respectively, upon cooling. Such phase transition corresponds to the structural transition from the HT-polymorph, which is orthorhombic, space group *Pnma*, and contains dynamic disorder of the dca and pyrazine ligands, to the LT-polymorph, that is monoclinic, space group $P2_1/n$ and where the dca and pyrazine ligands are ordered. Interestingly, these compounds display a dielectric anomaly associated to such phase transition, where the ε'_r values are small at low temperature and increase with temperature, showing an anomaly close to the phase transition temperature. From a detailed analysis of the LT- and HT-crystal structures, we have observed that the polar dca ligands, which bridge two transition metal cations, display a cooperative electrical arrangement. In fact, the crystal structure of these compounds is comprised of two interpenetrated networks, where the dipoles within each network show a ferroelectric (FE) arrangement. Nevertheless, the antiparallel stacking of the two interpenetrated FE networks gives rise to a net long-range antiferroelectric (AFE) order in these compounds. In this context, the "dynamic" disorder of the dca ligands in the HT-phase can sporadically break up the antiparallel arrangement of the electrical dipoles, giving rise to the anomaly in ε'_r observed at the phase transition. Very interestingly, the origin of such dielectric anomaly observed in the $M(dca)_2pyz$ compounds, is thus quite different from that observed in other hybrid inorganic-organic compounds, as in the here presented compounds, both the dielectric and magnetic response directly come from the framework. This finding is very interesting to obtain type II-multiferroic materials, with a strong coupling between both functional properties.

Acknowledgments

The authors are grateful for the financial support from Ministerio de Economía y Competitividad MINECO (MINECO) ENE2014-56237-C4-4-R and Xunta de Galicia under the project GRC2014/042.

References

---

[1] A. Kojima, K. Teshima, Y. Shirai, T. Miyasaka, J. Am. Chem. Soc. 131 (2009) 6050–1.

[2] X.-Y. Wang, L. Gan, S.-W. Zhang, S. Gao, Inorg. Chem. 43 (2004) 4615–25.

[3] P. Jain, N.S. Dalal, B.H. Toby, H.W. Kroto, A.K. Cheetham, J. Am. Chem. Soc. 130 (2008) 10450–1.

[4] P. Jain, V. Ramachandran, R.J. Clark, H.D. Zhou, B.H. Toby, N.S. Dalal, H.W. Kroto, A.K. Cheetham, J. Am. Chem. Soc. 131 (2009) 13625–7.

[5] J. F. Scott, Nat. Mater., 6 (2007) 256–257

[6] Y.-H. Chu, L.W. Martin, M.B. Holcomb, M. Gajek, S.-J. Han, Q. He, N. Balke, C.-H. Yang, D. Lee, W. Hu, Q. Zhan, P.-L. Yang, A. Fraile-Rodriguez, A. Scholl, S.X. Wang, R. Ramesh, Nat. Mater. 7 (2008) 478–482.

---

[7] Z. M. Wang, B. Zhang, T. Otsuka, K. Inoue, H. Kobayashi, M. Kurmoo, Dalt. Trans. 15 (2004) 2209-16.

[8] K.-L. Hu, M. Kurmoo, Z. Wang, S. Gao, Chem. Eur. J., 15 (2009) 12050–64.

[9] M. Mączka, A. Ciupa, A. Gągor, A. Sieradzki, A. Pikul, B. Macalik, M. Drozd, Inorg. Chem. 53 (2014) 5260–8.

[10] S. Chen, R. Shang, K.-L. Hu, Z.-M. Wang, S. Gao, Inorg. Chem. Front. 1 (2014) 83-93.

[11] R. Shang, G.-C. Xu, Z.-M. Wang, S. Gao, Chem. Eur. J. 20 (2014) 1146–58.

[12] M. Sánchez-Andújar, S. Presedo, S. Yáñez-Vilar, S. Castro-García, J. Shamir, M. A Señarís-Rodríguez, Inorg. Chem. 49 (2010) 1510–6.

[13] B. Pato-Doldán, L.C. Gómez-Aguirre, J.M. Bermúdez-García, M. Sánchez-Andújar, A. Fondado, J. Mira, S. Castro-García, M. A. Señarís-Rodríguez, RSC Adv. 3 (2013) 22404-11.

[14] A. Stroppa, P. Barone, P. Jain, J.M. Perez-Mato, S. Picozzi, Adv. Mater. 25 (2013) 2284–90.

[15] P. Jensen, S. R. Batten, B. Moubaraki, K. S. Murray, J. Solid State Chem. *159* (2001) 352–361.

[16] J.A. Schlueter, U. Geiser, J.L. Manson, J. Phys. IV. 114 (2004) 475–479.

[17] S.R. Batten, K.S. Murray, Coord. Chem. Rev. 246 (2003) 103–130.

[18] A.C. Larson, R.B. von Dreele*General Structure Analysis System (GSAS)*, Los Alamos National Laboratories, Report LAUR 86-748, 1990.

[19] J. R. Macdonald, LEVM version 8.0 Comlex Nonlinear Squares Fitting Program, 2003.

[20] C.N.R. Rao, K.J. Rao, *Phase transitions in solids*, Maidenhead (England), McGraw-Hill, 1978.

[21] M.Sánchez-Andújar, L. C. Gómez-Aguirre, B. Pato Doldán, S. Yáñez-Vilar, R. Artiaga, A. L. Llamas-Saiz, R. S. Manna, F. Schnelle, M. Lang, F. Ritter, A. A. Haghighirad, M. A. Señarís-Rodríguez, CrystEngComm 16 (2014) 3558.

[22] D. C. Sinclair, T. B. Adams, F. D. Morrison, A. R. West Appl. Phys. Lett., 80 (2002) 2153.

[23] (a) J. F. Scott, J. Phys.: Condens. Matter 20 (2008) 21001 (b) A. Loidl, S. Krohns, J. Hemberger, P. Lunkenheimer, J. Phys.: Condens. Matter 20 (2008) 19100.

---

[24] D. Khomskii, Physics 2 (2009) 20.

[25] S. Picozzi, A. Stroppa, Eur. Phys. J. B 85 (2012) 240.

FIGURE CAPTIONS

Fig. 1. Crystal structure of the M(dca)$_2$pyz compounds viewed along the c-axis (a) HT-phase and (b) LT-phase. To facilitate the visualization, the unit cells have been expanded and the [MN$_6$] octahedra of the interpenetrated networks have been labeled with different colors (cyan and red).

Fig. 2. SEM images of the obtained M(dca)$_2$pyz materials obtained under different magnifications.

Fig. 3.Room temperature PXRD patterns for the as-prepared M(dca)$_2$pyz (M:Fe^{2+}, Co^{2+}, Zn^{2+}) compounds and the simulated one based on the single crystal data at room temperature.

Fig. 4. TGA curves of the M(dca)$_2$pyz (M:Fe^{2+}, Co^{2+}, Zn^{2+}) materials obtained under N$_2$ atmosphere.

Fig. 5. DSC results as a function of temperature obtained by heating and cooling the samplesM(dca)$_2$pyz (M:Fe^{2+}, Co^{2+}, Zn^{2+}) at a rate of 10 K/min. a) M=Fe^{2+}, b) M=Co^{2+} and c) M=Zn^{2+}.

Fig. 6. Temperature dependence of the dielectric constant, ε'_r of M(dca)$_2$pyz compounds measured at different frequencies (f=10–40 kHz), a) M=Fe^{2+}, b) M=Co^{2+} and c) M=Zn^{2+}.Additionally, we have highlighted with different colors the temperature regions, where each of the polymorphs is stable: (cyan) for the HT-phase and (yellow) for the LT-phase.

Fig. 7. Crystal structure of the HT-phase viewed along the *b*-axis and of the LT-phase viewed along the *a*-axis. To facilitate the visualization, each of the subnetworks has been drawn in different colors (cyan and red) and the pyzarine ligands have been removed. The arrows show the electrical dipole of the dca ligands.

se

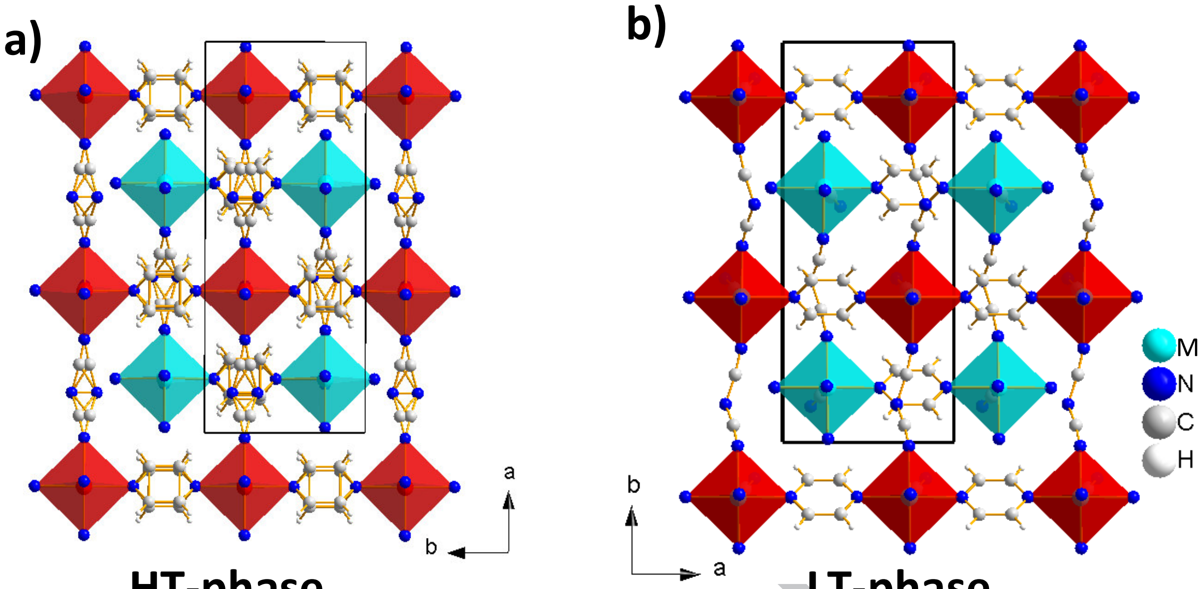

HT-phase

LT-phase

Fig. 1

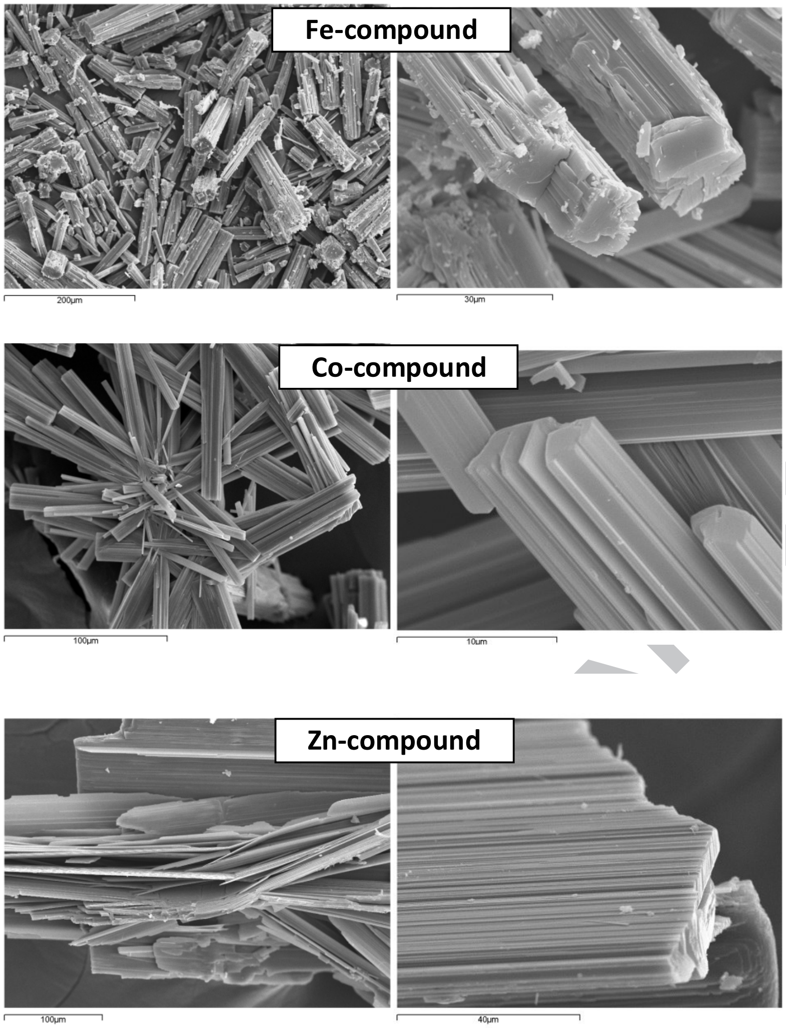
Fe-compound
200µm
30µm
Co-compound
100µm
10µm
Zn-compound
100µm
40µm

Fig. 2

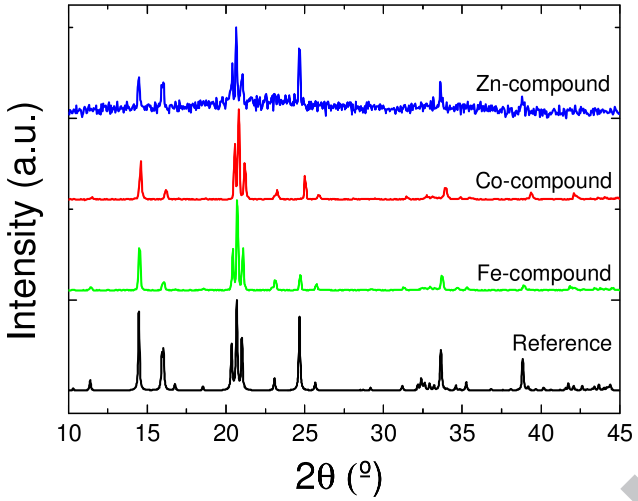
Zn-compound
Co-compound
Fe-compound
Reference
Intensity (a.u.)
10
15
20
25
30
35
40
45
2θ (º)

Fig. 3

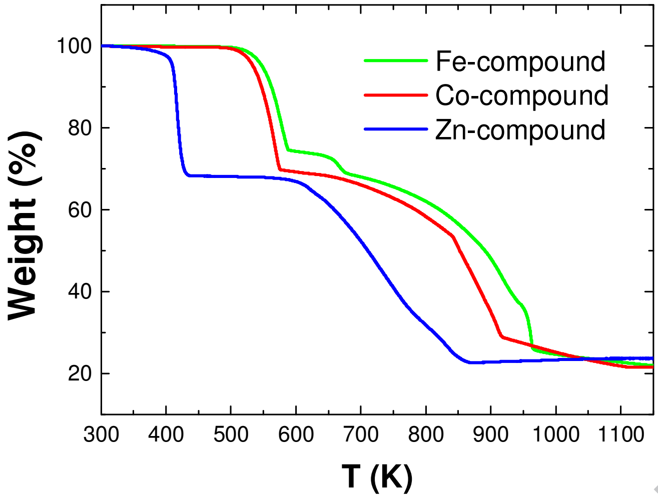
Weight (%)
100
80
60
40
20
300
400
500
600
700
800
900
1000
1100
T (K)
Fe-compound
Co-compound
Zn-compound

Fig. 4

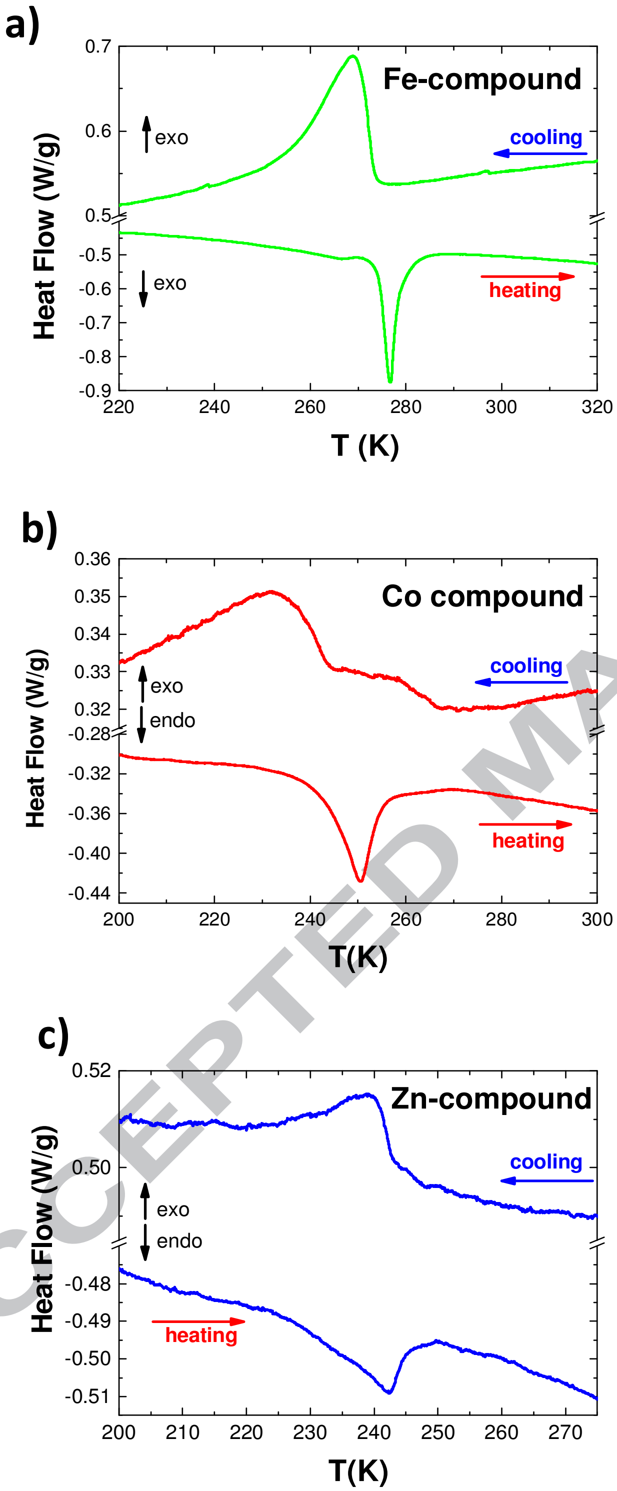
a)
Fe-compound
0.7
0.6
0.5
-0.5
-0.6
-0.7
-0.8
-0.9
exo
exo
cooling
heating
Heat Flow (W/g)
220
240
260
280
300
320
T (K)
b)
Co compound
0.36
0.35
0.34
0.33
0.32
-0.28
-0.32
-0.36
-0.40
-0.44
exo
endo
cooling
heating
Heat Flow (W/g)
200
220
240
260
280
300
T(K)
c)
Zn-compound
0.52
0.50
-0.48
-0.49
-0.50
-0.51
exo
endo
cooling
heating
Heat Flow (W/g)
200
210
220
230
240
250
260
270
T(K)

Fig. 5

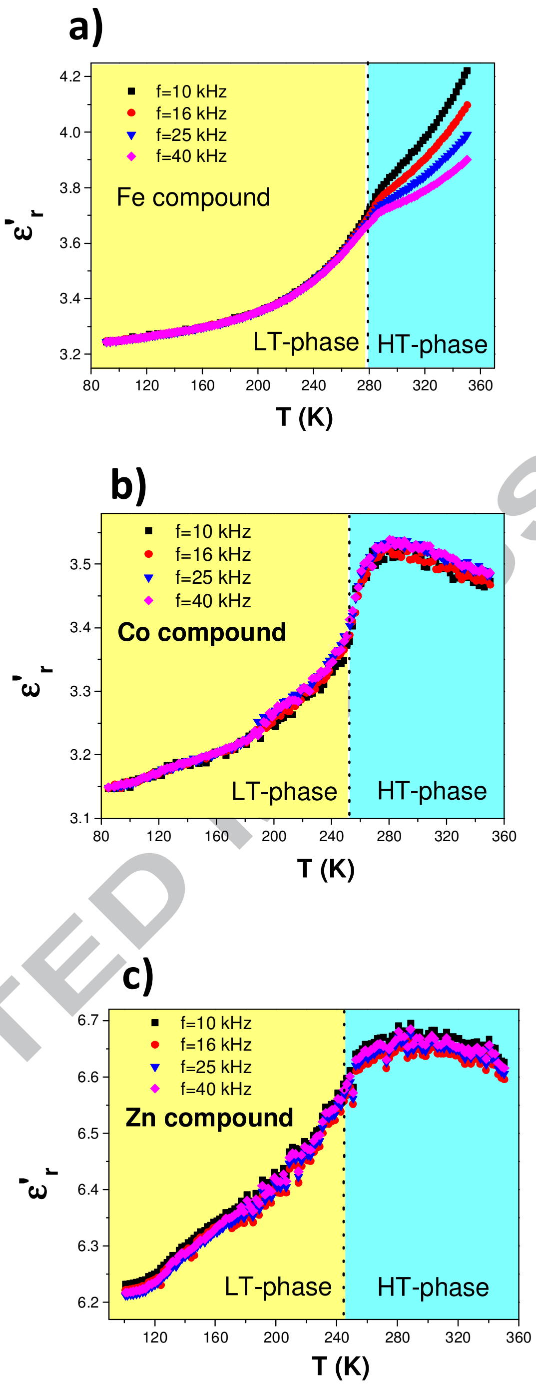
a)
f=10 kHz
f=16 kHz
f=25 kHz
f=40 kHz
Fe compound
LT-phase
HT-phase
ε'_r
4.2
4.0
3.8
3.6
3.4
3.2
80
120
160
200
240
280
320
360
T (K)
b)
f=10 kHz
f=16 kHz
f=25 kHz
f=40 kHz
Co compound
LT-phase
HT-phase
ε'_r
3.5
3.4
3.3
3.2
3.1
80
120
160
200
240
280
320
360
T (K)
c)
f=10 kHz
f=16 kHz
f=25 kHz
f=40 kHz
Zn compound
LT-phase
HT-phase
ε'_r
6.7
6.6
6.5
6.4
6.3
6.2
120
160
200
240
280
320
360
T (K)

Fig. 6

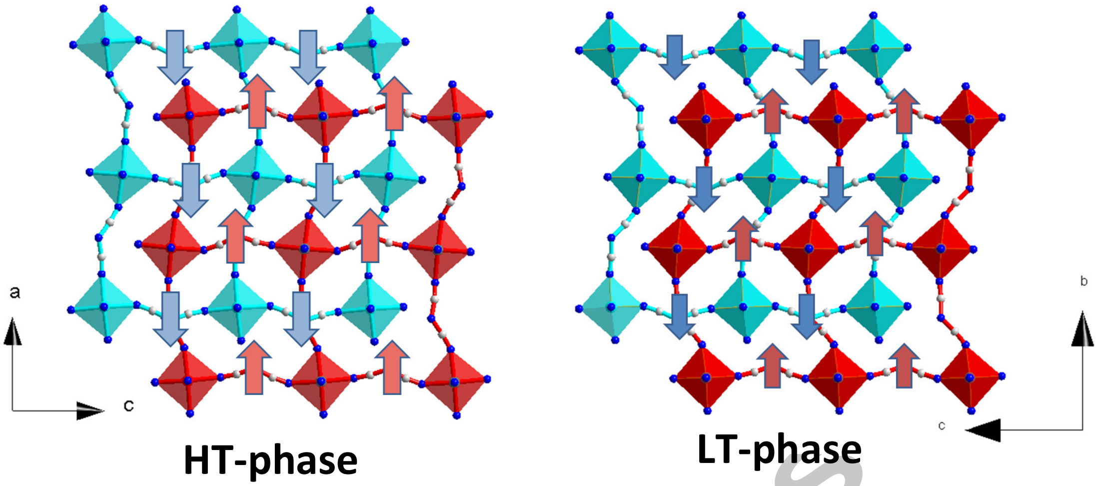

Fig. 7

TABLE CAPTION

Table 1.- Cell parameters of the M(dca)$_2$pyz (M:Fe^{2+}, Co^{2+}, Zn^{2+}) compounds and agreement factors obtained from the LeBail refinement of their PXRD patterns at room temperature.

Compound	**a (Å)**	**b (Å)**	**c (Å)**	**R_{wp}**	**R_p**	**χ^2**
Fe	17.216(2)	7.227(1)	8.729(1)	20.44	11.71	1.82
Co	17.043(3)	7.106(1)	8.623(1)	19.79	12.03	1.41
Zn	17.154(3)	7.201(2)	8.695(2)	28.24	20.68	1.33

Table 1

GRAPHICAL ABSTRATS

Pictogram:

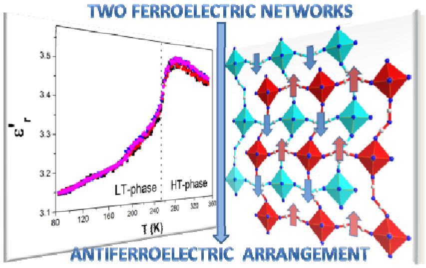

GRAPHICAL ABSTRATS

Synopsis:

The hybrid organic-inorganic M(dca)$_2$pyz compounds display a crystal structure comprised of two interpenetrated networks, where each net displays a ferroelectric (FE) arrangement of the polar dicyanamide (dca) anions. Both FE subnets showed an antiferroelectric arrangement. Very interestingly, the polar dca anions are involves at magnetic and electric arrangement that is interesting for obtain magnetoelectric coupling.